Pergamon

Geochimica et Cosmochimica Acta, Vol. 62, No. 11, pp. 1985–1991, 1998

0016-7037/98 $19.00 + .00

PII S0016-7037(98)00123-9

Multicomponent diffusion and convection in molten MgO-Al_2O_3-SiO_2

FRANK M. RICHTER,[1,*] YAN LIANG,[1,2] and WILLIAM G. MINARIK[3,†]

[1]Department of the Geophysical Sciences, The University of Chicago, 5734 South Ellis Avenue, Chicago, Illinois 60637, USA
[2]Department of Earth and Environmental Sciences, Rensselaer Polytechnic Institute, Troy, New York 12180, USA
[3]Institute for Geophysics and Planetary Physics, Lawrence Livermore National Laboratory, Livermore, California 94551, USA

(*Received August* 12, 1997; *accepted in revised form March* 5, 1998)

Abstract—Multicomponent diffusion and convection in molten MgO-Al_2O_3-SiO_2 at 1550°C and 0.5 GPa were examined experimentally in diffusion couples formed around 22.5 (wt%) MgO, 17.5% Al_2O_3, and 60% SiO_2. The diffusion matrix obtained from a simultaneous least squares inversion of convectively stable intersecting chemical diffusion profiles has large off-diagonal terms indicating, for example, very strong coupling of the flux of SiO_2 with gradients in MgO. In contrast to an earlier report on multicomponent diffusion involving the same compositions studied here, we found no features along the stable diffusion profiles that could not be explained in terms of a 2 × 2 diffusion matrix. X-ray concentration maps of the sectioned diffusion charges showed that double-diffusive convection had occurred in a number of experiments along the direction of constant SiO_2, even though the more dense melt had been placed below the less dense composition. The occurrence of such double-diffusive fingering instabilities is shown to be consistent with the predictions of linear stability theory. *Copyright © 1998 Elsevier Science Ltd*

1. INTRODUCTION

Diffusion and advection are the two types of mass transfer in the continuum representation of conservation of mass of each component in a multicomponent system. The formal distinction between diffusion and advection is not a matter of identifying each with a particular mechanism, but rather depends on the frame of reference used for measuring fluxes and how one chooses to define the advective velocity. Once the advective velocity is specified, diffusion represents that part of the flux not accounted for by advection. Definitions of advective or convective velocity and diffusive flux under various choices of reference frame (e.g., mass-fixed, volume-fixed, solvent-fixed) as well as relations for transforming from one reference frame to another can be found in, among others, Kirkwood et al. (1960), de Groot and Mazur (1962), Haase (1969), and Miller et al. (1986). In a mass-fixed (barycentric) frame of reference (adopted in this study), for example, the advective velocity, $\mathbf{u}$, of an n-component fluid is defined by

$$\mathbf{u} = \sum_{k=1}^{n} C_k \mathbf{u}_k, \tag{1}$$

where $C_k = \rho_k/\rho$ is the mass fraction of component k, $\mathbf{u}_k$ is the velocity associated with the total flux of k, ρ_k is the concentration (mass per unit volume) of k, and ρ is the local fluid density. The diffusive flux of component k, $\mathbf{J}_k$, relative to the local center of mass is then

$$\mathbf{J}_k = \rho C_k(\mathbf{u}_k - \mathbf{u}) \tag{2}$$

and in the absence of sources or sinks, mass conservation of component k takes the form (e.g., de Groot and Mazur, 1962)

$$\rho \frac{\partial C_k}{\partial t} + \rho \mathbf{u} \cdot \nabla C_k + -\nabla \cdot \mathbf{J}_k. \tag{3}$$

There is a long-standing tradition (e.g., Onsager, 1945; de Groot and Mazur, 1962; Haase, 1969) of assuming that the diffusive flux of k in an n-component isothermal nonreacting fluid can be related to concentration via a constituitive equation involving a linear combination of concentration gradients of the form

$$\mathbf{J}_k = -\rho \sum_{j=1}^{n-1} D_{kj}^n \nabla C_j, \tag{4}$$

where D_{kj}^n are elements of an $(n-1) \times (n-1)$ diffusion matrix with component n taken as the dependent component. The summation in Eqn. 4 is over only $n-1$ components because the concentration of the nth component can always be replaced by a linear combination of the other $n-1$ components. The best choice of the dependent component depends on the problem of interest (e.g., Miller et al., 1986; Liang et al., 1994, 1996). Substituting Eqn. 4 into Eqn. 3 gives

$$\rho \frac{\partial C_k}{\partial t} + \rho \mathbf{u} \cdot \nabla C_k = \sum_{j=1}^{n-1} \nabla \cdot (\rho D_{kj}^n \nabla C_j). \tag{5}$$

In many practical applications, the density and composition variations in a fluid system are small, in which case Eqn. 5 can be further simplified by neglecting the divergence of ρD_{kj}^n. The neglected terms are of order $\nabla D_{kj}^n/D$ and $\Delta\rho/\rho_O$, where ∇D_{kj}^n and $\Delta\rho$ are the magnitude of diffusivity and density variations in the fluid, respectively, D is a characteristic diffusivity, and ρ_O is the average density. This type of simplification is in essence an extension of the Boussinesq approximation, a stan-

*Author to whom correspondence should be addressed (richter@geosci.uchicago.edu).
†*Present address:* Geophysical Laboratory, Carnegie Institution of Washington, 5240 Broad Branch Road, NW, Washington, DC 20010, USA.

dard procedure in dealing with many heat and mass transfer problems. The resulting diffusion-advection equation is

$$\frac{\partial C_k}{\partial t} + \mathbf{u} \cdot \nabla C_k = \sum_{j=1}^{n-1} D_{kj}^n \nabla^2 C_j. \quad (6)$$

In the absence of convection (bulk flow driven by buoyancy forces), or more generally, in situations where the advective timescale is large compared to the diffusive timescale (UL/D $\ll$ 1, where U and L are characteristic velocity and length, respectively, and D is a measure of the diffusivity), Eqn. 6 reduces to

$$\frac{\partial C_k}{\partial t} = \sum_{j=1}^{n-1} D_{kj}^n \nabla^2 C_j. \quad (7)$$

Equations 6 and 7 are the two that we use below to discuss multicomponent diffusion and convection in molten MgO-Al_2O_3-SiO_2 (MAS). Preliminary results on diffusion in the CaO-MgO-Al_2O_3-SiO_2 (CMAS) system are also reported.

Constitutive equations of the form given by Eqn. 4 have long been thought to be appropriate representations for diffusive chemical fluxes in molten silicates based on the successful determination of the diffusion matrix for such systems as CaO-Al_2O_3-SiO_2 (Sagawara et al., 1977; Oishi et al., 1982; and more recently by Liang et al., 1996), K_2O-Al_2O_3-SiO_2 (Chakraborty et al., 1995), K_2O-SrO-SiO_2 (Varshneya and Cooper, 1972), and Na_2O-CaO-SiO_2 (Wakabayashi and Oishi, 1978, with diffusion matrix given by Trial and Spera, 1994).

The first report that we are aware of claiming that an $(n-1) \times (n-1)$ diffusion matrix might not be sufficient to account for diffusion in an n-component silicate melt is a paper by Kress and Ghiorso (1993) on multicomponent diffusion in molten MAS and CMAS. The specific features of the diffusion profiles reported by Kress and Ghiorso (1993) that cannot be explained by an $(n-1) \times (n-1)$ diffusion matrix are abrupt changes in the slope of the concentration gradients, most often in the vicinity of the original interface, leading these authors to conclude that "adequate representation of the complicated second-order features awaits a more appropriate mathematical formulation [than that given by equation (7)]."

The suggestion that a 2 × 2 (or 3 × 3) diffusion matrix might not be an adequate representation of chemical diffusion in a 3- (or 4-) component silicate melt (MAS or CMAS) is sufficiently striking in its implications (i.e., that a formalism that has been in use for more than 50 years is not a generally adequate representation of multicomponent diffusion) that we decided to repeat some of the experiments that led Kress and Ghiorso (1993) to make such a suggestion. We ran a series of chemical diffusion experiments in molten MAS at 1550°C and 0.5 GPa using diffusion couples having the same starting compositions (Table 1) as those used by Kress and Ghiorso (1993) in their ~1485°C, atmospheric pressure (1 atm) experiments. The reason that we used a higher pressure was to eliminate potentially mobile gas bubbles, which occur in 1 atm experiments (Kress and Ghiorso, 1993) but dissolve in the melt at 0.5 GPa. We used a slightly higher temperature (1550°C vs. 1485°C) to ensure that all our starting compositions would be molten at 0.5 GPa. A brief account of the experimental methods used in our study is given in the next section. The compositional variations in quenched diffusion couples are measured both as concentration profiles and as X-ray intensity maps. The X-ray concentration maps are especially useful in detecting convection of the sort that we have shown can exist in molten CAS even when a less dense melt is placed above a more dense melt (Liang et al., 1994; Liang, 1995). We found that convection occurred in many of the MAS diffusion couples and discuss this in terms of a linear stability theory based on the diffusion matrix obtained from only those chemical diffusion profiles that were not affected by convection. Our diffusion profiles that were not affected by convection did not show any of the abrupt changes in slope in the vicinity of the interface reported previously by Kress and Ghiorso (1993), thus we were able to find a 2 × 2 diffusion matrix for MAS that produces virtually perfect fits to all our stable diffusion profiles. We also show that chemical diffusion profiles in CMAS liquids are well fit using a 3 × 3 diffusion matrix.

Table 1. List of starting compositions (in wt%).

Sample	MgO	Al_2O_3	SiO_2	Density*
MAS1	24.65±0.06†	15.65±0.06	59.78±0.25	2.580
MAS2	19.59±0.12	20.62±0.10	59.96±0.12	2.560
MAS3	20.08±0.11	15.43±0.09	64.76±0.36	2.539
MAS4	24.96±0.08	20.31±0.09	55.17±0.37	2.605

*Densities (10^3 kg·m^{-3}) are at 1550°C and 0.5 GPa, calculated using the partial molar volume data of Lange and Carmichael (1990).
†±1σ errors are estimated from repeated analysis of homogeneous portions of the diffusion couples.

2. EXPERIMENTAL METHODS

Starting compositions, listed in Table 1, were synthesized from ultrapure MgO, Al_2O_3, and SiO_2 (Aldrich Chemical Co.) at 1455–1520°C and 1 atm. These compositions are within 1 wt% of those used by Kress and Ghiorso (1993) to make two of the four diffusion couples reported in their study. The two diffusion couples that we chose to replicate (MAS2-MAS1 and MAS4-MAS3) intersect at the common composition, 22.5 (wt)% MgO, 17.5% Al_2O_3, and 60% SiO_2, and for this reason are the most suitable for inverting to obtain a diffusion matrix. Diffusion couples were formed either by joining two previously synthesized uniform glass rods or by firmly packing two starting glass powders directly into holes drilled into a molybdenum capsule. Platinum sleeves are used to separate melt from the molybdenum sidewalls in experiments where we juxtaposed previously synthesized glass rods (Liang et al., 1994, 1996). When diffusion couples were made by directly loading glass powders, no platinum sleeve was used because electron microprobe measurements show that the extent of reaction between the melt and the molybdenum is negligibly small for the run durations of our present study. The diffusion (or in unstable situations, convection) experiments were carried out in a $^3/_4$" piston cylinder apparatus at 1550°C and 0.5 GPa in the same way as our earlier experiments in molten CAS (Liang et al., 1994, 1996). Diffusion profiles and X-ray concentration maps were collected from sectioned charges using a Cameca SX-50 electron microprobe at the University of Chicago and a JEOL 733 microprobe at the Lawrence Livermore National Laboratory. Representative concentration profiles of chemical diffusion are shown in Fig. 1 and false-color X-ray intensity maps of Al for two cases of convection are shown in Fig. 2.

3. RESULTS AND DISCUSSIONS

A total of eleven diffusion and convection experiments were run at 1550°C and 0.5 GPa (Table 2). ST-9 (MAS2/MAS1), a four hour run, suffered from temperature fluctuations and is not included in Table 2. To promote or suppress convection, cylindrical diffusion couples of different diameters (0.85–3.75 mm) were used and run for 6–240 min (Table 2). As one would

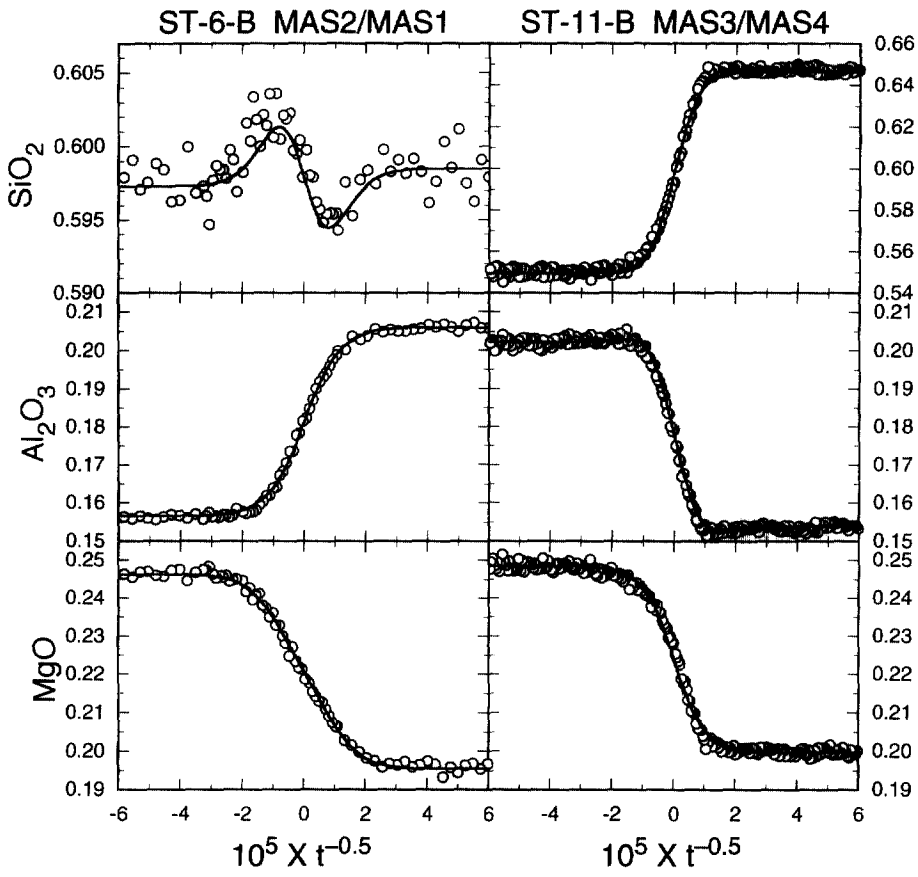

Fig. 1. Microprobe traverse (weight fractions, open circles) of the chemical diffusion runs along two compositional directions: MAS2/MAS1 (ST-6 B) and MAS3/MAS4 (ST-11 B) plotted against normalized distance with X in meters and time (t) in seconds. Solid lines are calculated diffusion profiles using the average diffusion matrix given in Table 3. Microprobe analyses used an accelerating voltage of 15 kV, a beam current of 25 nA, and a beam spot of 5 μm. Long counting times (30 seconds) were used to achieve high analytical accuracy, because the accuracy of the inverted diffusion matrix is very dependent on the accuracy with which the diffusion profiles are measured.

expect, convection was found to have occurred in runs ST-3 and ST-4 B using the couple MAS4/MAS3 (top-half/bottom-half) which was formed (accidentally) by placing the more dense melt above the less dense one. The three experiments with the less dense MAS3 composition placed above the more dense MAS4 (runs ST-11 A, ST-11 B and ST-14 A) showed no evidence of convection. Experiments using the couple MAS2/MAS1 were often found to have convected even though the less dense melt MAS2 was placed above the more dense melt MAS1. The most likely explanation is that couples MAS2/MAS1 are unstable to double-diffusive fingering instabilities in much the same way as we found earlier for CAS melts along the direction of constant SiO_2 (Liang et al., 1994; Liang, 1995). MAS2/MAS1 couples provide diffusion profiles unaffected by convection only when run for 60 min or less (runs ST-4 A, ST-5 B, ST-6 A, ST-6 B, and ST-7 A).

3.1. Diffusion Matrix

Table 3 gives four estimates (and their average) of the chemical diffusion matrix with SiO_2 as the dependent variable for a MAS liquid (22.5% MgO, 17.5% Al_2O_3, and 60% SiO_2, 1550°C, 0.5 GPa) obtained from a simultaneous least squares inversion of concentration profiles along two directions in the composition space (Liang, 1994; Liang et al., 1996). Figure 1a and b compares the diffusion profiles (solid lines) calculated using the average diffusion matrix given in Table 3 to the measured concentration data (open circles) from runs ST-6 B and ST-11 B. The consequences of significant off-diagonal terms, often negative, in the diffusion matrix (Table 3, and Table 4 when Al_2O_3 is taken as the dependent variable) are easily seen in the profiles shown in Fig. 1. For example, the SiO_2 profile in Fig. 1a shows that diffusion of SiO_2 has taken place even though it was initially uniform. This is clear evidence that the flux of SiO_2 must depend on more than just gradients in SiO_2, implying coupling to gradients in other components, which is represented by the off-diagonal term $D^{Al_2O_3}_{SiO_2-MgO}$ in the diffusion matrix given in Table 4. Since the flux of SiO_2 implied by the data in Fig. 1a is opposite to that of MgO, $D^{Al_2O_3}_{SiO_2-MgO}$ must be negative. Another effect of off-diagonal terms is seem if one compares the MgO profile in Fig. 1a to that in Fig. 1b. It is very obvious that MgO diffuses significantly faster when its flux is opposite to that of Al_2O_3. This directional (in composition space) dependence of the diffusion of MgO is a consequence of $D^{SiO_2}_{MgO-Al_2O_3}$ being negative (see Table 3).

Table 3 compares our measured diffusion matrix for MAS

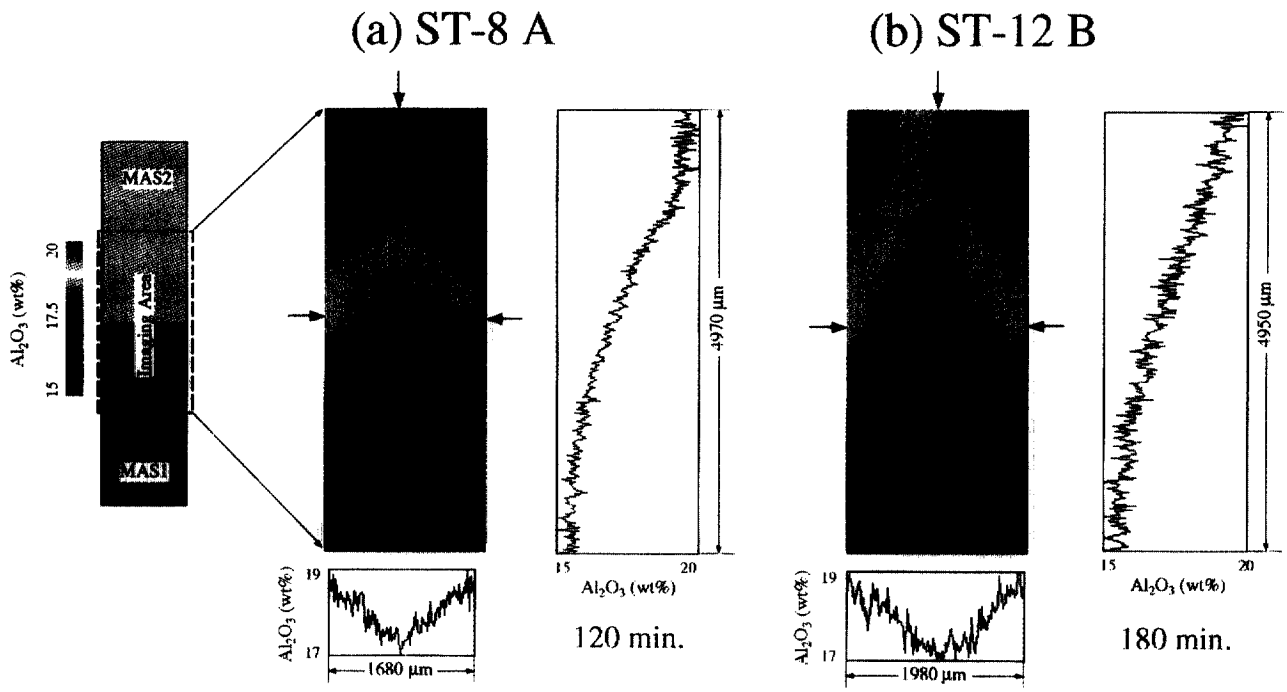

Fig. 2. False-colored X-ray intensity maps of the element Al showing double-diffusive fingering instabilities in runs ST-8 A (a), and ST-12 B (b). The ranges of compositional variations (converted to wt%) are represented by the vertical scale bar on the left of ST-8 A. The area where X-ray intensity maps were collected is shown in the schematic drawing of a diffusion couple by a dashed rectangle. The black strips on the sides of each image are the container walls. The arrows in (a) and (b) mark directions along which the two concentration profiles were obtained from each map. The X-ray intensity maps of Ca and Si were also collected, but the ones for Al have the best counting statistics. The X-ray intensities were collected using an electron microprobe with an accelerating voltage of 15 kV, a beam current of 100 nA, and a beam spot of 5 μm.

with that reported by Kress and Ghiorso (1993) for a nearly identical melt composition but at ~1485°C and 1 atm. The two diffusion matrices are significantly different in the sense that the differences are larger than our estimated errors. The differences between the diffusion matrices could be due to the different temperature and pressure of the experiments from which they were derived, but we hesitate to make such an interpretation because we believe that some of the diffusion profiles used by Kress and Ghiorso (1993) to obtain their diffusion matrix might have been affected by double-diffusive convection, and in any event often failed to give good fits to their measured diffusion profiles. Table 4 compares our measured diffusion matrix with that in CAS around the composition 25% CaO, 15% Al_2O_3, and 60% SiO_2 at 1500°C and 1 GPa (Liang et al., 1996). In spite of the differences in temperature, pressure, and composition between the two ternary systems, the behavior of SiO_2 is almost identical. In the case of molten CAS, we have already shown that the strong coupling of the flux of SiO_2 with gradients in CaO gives rise to fingering instabilities in diffusion couples formed along the direction of constant SiO_2 (Liang et al., 1994; Liang, 1995). The very similar coupling of SiO_2 with MgO leads to the expectation of similar instability in the MAS system.

Table 2. Summary of diffusion and convection runs.

Run	Hole number	Couple top/bottom	Diameter (mm)	Duration (minutes)	Comments
ST-3	A	MAS4/MAS3	1.30	24	down-going finger
ST-4	A	MAS2/MAS1	1.66	60	stable diffusion
ST-4	B	MAS4/MAS3	0.80	60	down-going finger
ST-5	B	MAS2/MAS1	3.75	30	stable diffusion
ST-6	A	MAS2/MAS1	1.47	30	stable diffusion
ST-6	B	MAS2/MAS1	0.94	30	stable diffusion
ST-7	A	MAS2/MAS1	0.85	60	stable diffusion
ST-8	A	MAS2/MAS1	1.70	120	up-going finger
ST-10	A	MAS2/MAS1	1.84	240	up-going finger
ST-11	A	MAS3/MAS4	1.27	6	stable diffusion
ST-11	B	MAS3/MAS4	0.85	6	stable diffusion
ST-12	A	MAS2/MAS1	1.30	180	up-going finger
ST-12	B	MAS2/MAS1	2.00	180	up-going finger
ST-14	A	MAS3/MAS4	1.80	24	stable diffusion

Table 3. List of chemical diffusion coefficients taking SiO_2 as the dependent variable*.

$D^{SiO_2}_{MgO\text{-}MgO}$	$D^{SiO_2}_{MgO\text{-}Al_2O_3}$	$D^{SiO_2}_{Al_2O_3\text{-}MgO}$	$D^{SiO_2}_{Al_2O_3\text{-}Al_2O_3}$	Couples Used
5.86±0.20†	-1.88±0.50	-1.93±0.20	3.09±0.50	ST-4 A + ST-11 A
6.01±0.07	-1.76±0.05	-2.32±0.03	2.91±0.02	ST-4 A + ST-11 B
6.08±0.04	-2.02±0.04	-2.00±0.01	3.12±0.01	ST-6 B + ST-11 A
6.17±0.10	-1.88±0.07	-2.39±0.04	2.98±0.02	ST-6 B + ST-11 B
6.03±0.13‡	-1.88±0.11	-2.16±0.23	3.02±0.10	Average of the four
5.15§	-3.18	-2.48	4.45	Kress & Ghiorso

* Diffusion coefficients are in $\times 10^{-11}$ m^2s^{-1}; †±1 σ errors are quoted directly from each inversion. ‡±1 σ errors for the average are calculated from the measured diffusivities using the standard definition. § The diffusion matrix of Kress and Ghiorso (1993) is converted to a system where concentrations are in weight fraction (*cf.* eqns (139) and (140) on page 260 of de Groot and Mazur (1962)), while neglecting density variations across the diffusion couples.

Table 4. Comparisons between the unstable diffusion couples in molten MgO-Al_2O_3-SiO_2 and CaO-Al_2O_3-SiO_2.

	MAS 1550°C & 0.5 GPa	CAS 1500°C & 1 GPa†
D^3_{11} *	7.91	4.66
D^3_{12}	1.88	0.44
D^3_{21}	-2.73	-2.68
D^3_{22}	1.14	1.00
λ_a/λ_b	3.503	3.171
ρ_o	2.570	2.639
α_1	0.148	0.179
α_2	-0.193	-0.209
μ	0.3~1.6	4.5
ΔC_1	5%	10%
ΔC_2	-5%	-10%
ΔC_3	0	0

* Component 1 stands for MgO or CaO, 2 for SiO_2, and 3 for Al_2O_3. Superscript 3 denotes that Al_2O_3 is taken as a dependent variable for the diffusion matrix [D]. λ_a and λ_b are the major and minor eigenvalues of [D], respectively. Diffusion coefficients are in 10^{-11} m^2s^{-1}; density is in 10^3 $kg{\cdot}m^{-3}$; viscosity μ is in Pa·s. †[D] for CAS is from Liang et al., 1996. α_1 and α_2 are coefficients in the density-composition relation as defined in the text. ΔC_i is the difference in the concentration of component i between the end members of the diffusion couple.

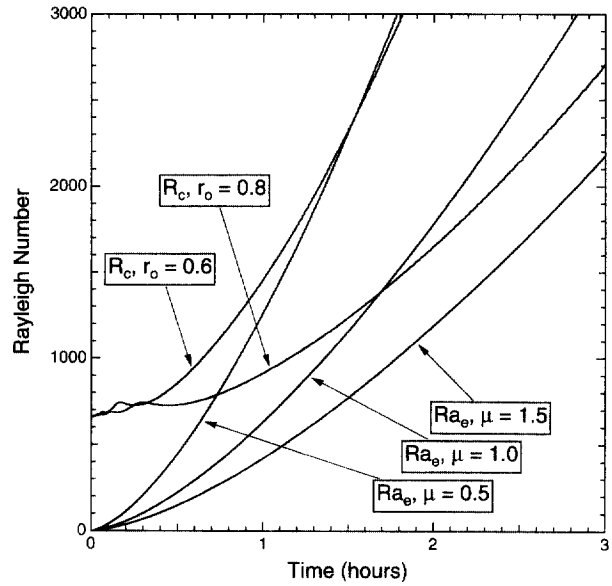

Fig. 3. Curves labelled R_c, r_o show the critical Rayleigh number R_c for the onset of the axisymmetric fingering instability as a function of time for two choices of the container diameter (r_o = 0.5 and 0.8 mm). Three curves of the effective Rayleigh number Ra_e for the diffusion couple MAS2/MAS1 were calculated using the data provided in Table 4 for three choices of melt viscosity (μ = 0.5, 1.0, and 1.5 Pa · s). For a given choice of r_o and μ, fingering instabilities grow in amplitude once $Ra_e > R_c$.

3.2. Double-Diffusive Convection

Figure 2a and b are false-color concentration maps of Al from diffusion couple MAS2/MAS1 in runs ST-8 A (two hours) and ST-12 B (three hours) each showing an approximately axisymmetric upward-moving convective "finger" of the less Al_2O_3-rich melt. The fingering instabilities observed in diffusion couples MAS2/MAS1 run for more than one hour are very similar to what we have previously found in CAS diffusion couples with similar Al_2O_3 and SiO_2 abundance run at 1500°C and 1 GPa (Liang et al., 1994; Liang, 1995). Table 4 reveals further similarities between the unstable CAS and MAS diffusion couples by comparing their diffusion matrices, density-composition relations, viscosities, and composition variations. The fingering instability of molten CAS along the constant SiO_2 direction can be explained in terms of the strong coupling of the flux of SiO_2 with gradients in CaO ($D^{Al_2O_3}_{SiO_2-CaO} = -2.68 \times 10^{-11}$ m^2s^{-1}), and in the MAS case we find virtually the same coupling between SiO_2 and MgO ($D^{Al_2O_3}_{SiO_2-MgO} = -2.73 \times 10^{-11}$ m^2s^{-1}).

Linear stability analysis (Liang, 1995) of a volume of ternary melt with constant concentration gradients confined in a vertical cylindrical container and free upper and lower boundary conditions shows that an axisymmetric fingering instability will grow in amplitude once the effective Rayleigh number Ra_e of the system exceeds a critical value R_c which is a function of the aspect ratio of the container ($\Gamma = r_o/d$), that is

$$Ra_e = \frac{g\,d^3}{\nu}\begin{bmatrix}\alpha_1\\ \alpha_2\end{bmatrix}^T\begin{bmatrix}D_{11} & D_{12}\\ D_{21} & D_{22}\end{bmatrix}^{-1}\begin{bmatrix}\nabla C_1\\ \nabla C_2\end{bmatrix} > R_c(\Gamma) \qquad (8)$$

where r_o is the radius of the cylindrical container, d is the thickness of the diffusive layer between the two melts, g is the acceleration of gravity, and ν is the kinematic viscosity of the melt. The superscript T stands for the transpose, subscripts 1 and 2 designate any two independent components in the melt, D_{ij} (i,j = 1,2) are the elements of diffusion matrix, ΔC_i is the concentration difference of i (in weight fraction) between the endmember compositions, and α_1, α_2 are coefficients in the linearized density-composition relation

$$\rho = \rho_o[1 + ga_1(C_1 - C_1^0) + \alpha_2(C_2 - C_2^0)] \qquad (9)$$

with C_i^0 the average concentrations of the system as a whole. Details regarding the dependence of the critical Rayleigh number $R_c(\Gamma)$ on the aspect ratio of the region of chemical gradients can be found in Liang (1995). $R_c(\Gamma)$ is a decreasing function of Γ, with a minimum value of 657.5 for $\Gamma \to \infty$. To use Eqn. 8 as the linear stability criteria for a chemically diffusing ternary system, we make the simplifying assumption that diffusion is sufficiently slow that we can test for stability ignoring the fact that the system is actually evolving slowly in time. The thickness d of the diffusive layer as a function of run time t can be estimated using the relation $d \approx 2\sqrt{\lambda_a \cdot t}$, where λ_a is the major eigenvalue of the diffusion matrix, and the aspect ratio Γ is then approximately $r_o/2\sqrt{\lambda_a \cdot t}$. Thus, both R_c and Ra_e are functions of experimental run time, with R_c increasing as the aspect ratio gets smaller with time, while the absolute magnitude of Ra_e increases as d^3.

Table 4 gives all the properties of the MAS system required to carry out a stability analysis for the case of a less dense melt above a more dense melt. Figure 3 displays the critical Rayleigh numbers R_c for the onset of the axisymmetric fingering instability as a function of time for two choices of capsule

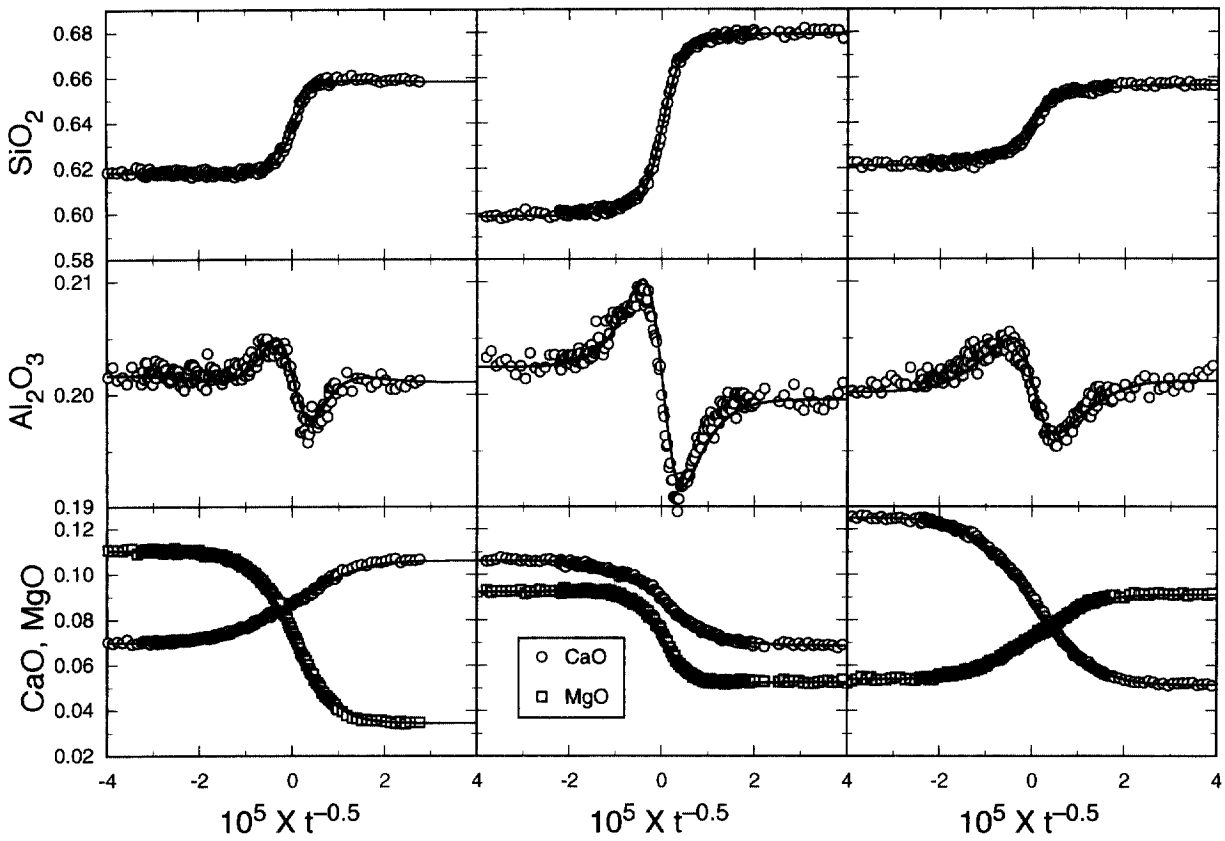

Fig. 4. Concentration profiles (weight fractions, open squares and open circles) of three chemical diffusion couples in molten CaO-MgO-Al_2O_3-SiO_2. The three diffusion couples were run in a three-hole molybdenum capsule at 1500°C and 1 GPa for 2.5 hours. These diffusion couples intersect at 8.8 (wt)% CaO, 7.2% MgO, 20.1% Al_2O_3, and 63.9% SiO_2 in composition space. Solid lines are the calculated diffusion profiles using a diffusion matrix (with Al_2O_3 as the dependent component) obtained by a simultaneous inversion of the diffusion profiles from all three couples using the Boltzmann-Matano method. The diffusion coefficients are (in 10^{-11} m^2s^{-1}):

$$D^{Al_2O_3}_{CaO-CaO} = 6.49 \qquad D^{Al_2O_3}_{CaO-MgO} = 0.66 \qquad D^{Al_2O_3}_{CaO-SiO_2} = 1.00$$

$$D^{Al_2O_3}_{MgO-CaO} = -0.95 \qquad D^{Al_2O_3}_{MgO-MgO} = 2.83 \qquad D^{Al_2O_3}_{MgO-SiO_2} = 0.52$$

$$D^{Al_2O_3}_{SiO_2-CaO} = -2.50 \qquad D^{Al_2O_3}_{SiO_2-MgO} = -1.40 \qquad D^{Al_2O_3}_{SiO_2-SiO_2} = -0.38$$

The concentration profiles were collected at the University of Chicago using a JEOL JSM-5800LV SEM equipped with an Oxford Link ISIS-300 X-ray microanalysis system. The analyses were run at an accelerating voltage of 15 kV and a beam current of 15 nA. Mineral standards were used and corrections made using the ZAF method.

radius (r_o = 0.5 and 0.8 mm). Also plotted in Fig. 3 are the effective Rayleigh number Ra_e for the diffusion couple MAS2/MAS1 calculated using the values given in Table 4 for three choices of melt viscosity (μ = 0.5, 1.0, and 1.5 Pa · s) lying between the viscosities of the endmember compositions. At the onset of an experiment, d = 0; therefore, Ra_e = 0 and R_c = 657.5 ($\Gamma \rightarrow \infty$). Both Ra_e and R_c increase with increasing time, with the actual trajectory of R_c depending on the radius of the capsule. The onset time for convection is given by the intersection of the appropriate Ra_e curve (depending on the choice of viscosity) with the appropriate (depending on the radius of the cylindrical container) R_c curve. Figure 3 shows that diffusion couples MAS2/MAS1 can be stable or unstable depending on the radius of the cylindrical container, the effective viscosity of the melt, and the duration of the run. All the stable and unstable experiments listed in Table 2 for diffusion couple MAS2/MAS1 are consistent with the linear stability analysis when the effective viscosity of the melt is 1.0 Pa · s. As Fig. 3 predicts for μ = 1.0 Pa · s, all experiments with run times up to one hour showed no sign of convection while all those run for two hours or more did convect. The linear stability analysis of diffusion couple MAS3/MAS4 shows that it is always stable against convection.

4. SUMMARY AND CONCLUSION

We undertook the multicomponent diffusion and convection experiments in MAS liquids listed in Table 2 with two main purposes in mind. First, these experiments are a natural extension of our earlier work on diffusion (Liang et at., 1996) and convection (Liang et al., 1994; Liang, 1995) in CAS liquids, and necessary precursors to experiments we are now completing in CMAS liquids. As can be seen by comparing the diffusion matrices of MAS and CAS given in Table 4, Ca and Mg

are very similar in the degree to which they affect and are affected by gradients in SiO_2 and Al_2O_3. Given the similarity of the MAS and CAS diffusion matrices and the other properties listed in Table 4, it is not surprising that these two systems are also very similar with regards to their tendency to convect. Our second purpose was to check the suggestion of Kress and Ghiorso (1993) that the traditional representation of multicomponent diffusion in terms of a diffusion matrix relating the flux of an independent component to gradients of all the independent components might not be an adequate representation of multicomponent diffusion in MAS and CMAS melts.

We concentrated our diffusion experiments on two directions in MAS composition space, one of these corresponding to the diffusion couples for which Kress and Ghiorso (1993) provide the most information (MAS2/MAS1) and which exhibited features not explainable by a traditional diffusion matrix; the second direction (MAS3/MAS4) being chosen because it intersects the first at a common composition half way between the endmembers of each. To avoid problems with migrating gas bubbles, all our experiments were run at 0.5 GPa and 1550°C, instead of 1 atm pressure and temperatures slightly below 1500°C used by Kress and Ghiorso (1993). We found that the diffusion profiles measured in MAS3/MAS4 couples, and MAS2/MAS1 couples run for one hour or less, could be fully accounted for by the diffusion matrix given in Table 3. However, diffusion couples MAS2/MAS1 run for two hours or more showed clear evidence of double-diffusive convection, even though the more dense composition was placed below the less dense one. We showed that the onset of such convection after about one hour is consistent with linear stability theory.

Applying the same linear stability analysis, but with the container dimensions of the experiments of Kress and Ghiorso (1993) and their diffusion matrix confirms their statement that all their MAS2/MAS1 couples are predicted to be stable with regards to convection. However, this conclusion is very sensitive to the diffusion matrix used in the analysis. For example, changing the value of the diffusion matrix elements by a few tens of percent can result in a prediction of these same couples being unstable. This suggests that the MAS2/MAS1 experiments of Kress and Ghiorso (1993) were very close to the stability boundary and might well have convected. Convection, however, does not in any simple way explain the peculiar changes in concentration gradients near the interface observed by Kress and Ghiorso (1993), and which led them to question the applicability of traditional diffusion matrices to molten silicates. As shown by the concentration profiles and concentration maps in Fig. 2, convection will displace and distort the concentration gradients, but it does not cause locally abrupt changes in their slope. So, the best that we can say is that we did not reproduce the peculiar changes in slope of the concentration gradients reported by Kress and Ghiorso (1993), and therefore found no evidence that would lead us to question the applicability of a 2×2 diffusion matrix to represent multicomponent diffusion in molten MAS.

We have not attempted to exactly duplicate any of the diffusion experiments of Kress and Ghiorso (1993) in the CMAS system, where they also sometimes found features that could not be explained by a traditional diffusion matrix. We are, for other reasons, presently engaged in an experimental study of multicomponent diffusion in CMAS, and so far we have not seen any features in the diffusion profiles that cannot be fully accounted for by a 3×3 diffusion matrix. Figure 4 is typical of our results to date and shows that a 3×3 diffusion matrix can reproduce the measured diffusion data from a number of different directions in composition space with very high precision.

Acknowledgments—We thank E. Bruce Watson for the use of experimental facilities and for many discussions during all stages of this project. We also thank Andrew M. Davis for providing chemical analysis of the diffusion runs reported in Fig. 4. This work was supported by DOE grant DE-FG02-94ER14478 to F. M. Richter. The experimental facilities we used at RPI are supported by NSF grant EAR-940691 to E. B. Watson, while those used at Lawrence Livermore National Laboratory are supported by the Institute for Geophysics and Planetary Physics under DOE contract W-7405-Eng-48.

REFERENCES

Chakraborty S., Dingwell D. B., and Rubie D. (1995) Multicomponent diffusion in ternary silicate melts in the system K_2O-Al_2O_3-SiO_2: I. Experimental measurements. *Geochim. Cosmochim. Acta* **59,** 255–264.

de Groot S. R. and Mazur P. (1962) *Non-Equilibrium Thermodynamics.* Dover.

Haase R. (1969) *Thermodynamics of Irreversible Processes.* Dover.

Kirkwood J. G., Baldwin R. L., Dunlop P. J., Gosting L. J., and Kegeles G. (1960) Flow equations and frame of reference for isothermal diffusion in liquids. *J. Chem. Phys.* **33,** 1505–1513.

Kress V. C. and Ghiorso M. S. (1993) Multicomponent diffusion in MgO-Al_2O_3-SiO_2 and CaO-MgO-Al_2O_3-SiO_2 melts. *Geochim. Cosmochim. Acta* **57,** 4453–4466.

Lange R. A. and Carmichael I. S. E. (1990) Thermodynamic properties of silicate liquids with emphasis on density, thermal expansion and compressibility. In *Modern Methods of Igneous Petrology* (ed. J. Nicholls and J. K. Russell); *Rev. Mineral.* **24,** 25–64.

Liang Y. (1994) Models and experiments for multicomponent chemical diffusion in molten silicates. Ph.D. dissertation, Univ. Chicago.

Liang Y. (1995) Axisymmetric double-diffusive convection in a cylindrical container: Linear stability analysis with applications to molten CaO-SiO_2-Al_2O_3. In *Double-Diffusive Convection* (ed. A Brandt and J. Fernando); *AGU Geophys. Monogr. Ser.* **94,** pp. 115–124.

Liang Y., Richter F. M., and Watson E. B. (1994) Convection in multicomponent silicate melts driven by coupled diffusion. *Nature* **369,** 390–392.

Liang Y., Richter F. M., and Watson E. B. (1996) Diffusion in silicate melts: II. Multicomponent diffusion in CaO-SiO_2-Al_2O_3 at 1500°C and 1 GPa. *Geochim. Cosmochim. Acta* **60,** 5021–5035.

Miller D. G., Vitagliano V., and Sartorio R. (1986) Some comments on multicomponent diffusion: Negative main term diffusion coefficients, second law constrains, solvent choices, and reference frame. *J. Phys. Chem.* **90,** 1509–1519.

Oishi Y., Nanba M., and Pask J. A. (1982) Analysis of liquid-state interdiffusion in the system CaO-Al_2O_3-SiO_2 using multiatomic ion models. *J. Amer. Ceram. Soc.* **65,** 247–253.

Onsager L. (1945) Theories and problems of liquid diffusion. *Ann. New York Acad. Sci.* **46,** 241–265.

Sugawara H., Nagata K., and Goto K. S. (1977) Interdiffusivities matrix of CaO-Al_2O_3-SiO_2 melt at 1723 K to 1823 K. *Metall. Trans.* **8B,** 605–612.

Trial A. F. and Spera F. J. (1994) Measuring the multicomponent diffusion matrix: Experimental design and data analysis for silicate melts. *Geochim. Cosochim Acta* **58,** 3769–3783.

Varshneya A. K. and Cooper A. R. (1972) Diffusion in the system K_2O-SrO-SiO_2: III. Interdiffusion coefficients. *J. Amer. Ceram. Soc.* **55,** 312–317.

Wakabayashi H. and Oishi Y. (1978) Liquid-state diffusion of Na_2O-CaO-SiO_2 system. *J. Chem. Phys.* **68,** 2046–2052.